Journal of Applied Sciences

ISSN 1812-5654

science alert

ANSInet
an open access publisher
http://ansinet.com

Journal of Applied Sciences 11 (11): 1885-1894, 2011
ISSN 1812-5654 / DOI: 10.3923/jas.2011.1885.1894

Generating Gas Turbine Component Maps Relying on Partially Known Overall System Characteristics

A.L. Tamiru, F.M. Hashim and C. Rangkuti
Department of Mechanical Engineering, Universiti Teknologi PETRONAS,
Bandar Seri Iskandar, 31750, Tronoh, Perak, Malaysia

Abstract: This study presents the result of an attempt to develop compressor and turbine maps for a 5.2 MW rated industrial gas turbine. The research is motivated by the need to study load accepting and load rejection characteristics of cooperating gas turbines. Only overall performance parameters of the gas turbine are provided by the manufacture and that made it difficult to carry out such studies. This work proposes the use of scaling method in the fixed geometry region and stage-stacking method in the variable geometry region. Generalized stage and overall component performance curves, all from literature, are used in presenting the performance maps. Characteristics of compressors whose actual maps are known are first used to choose a reference map. Relying on the selected map, predicted performance curves are obtained for the aforesaid gas turbine. The variable geometry is demonstrated considering actual data from literature. Having the design point parameters from limited overall performance data, the proposed approach has managed to get the key performance maps. The results can be used for stability, performance optimization and condition monitoring studies.

Key words: Gas turbine, performance map, scaling method, stage-stacking

INTRODUCTION

A gas turbine as part of a cogeneration plant delivers power at constant shaft speed and hot exhaust gas at optimum heat recovery steam boiler inlet temperature from the combustion of a gas or liquid fuel. Main components of a typical single-shaft gas turbine are as indicated in Fig. 1. The corresponding process diagram is given in Fig. 2. The air from the atmosphere is first compressed (process 1-2) to high pressure in the compressor. The compressed air is then mixed with fuel and burned (process 2-3') in the combustion chamber. The hot gas then expands through the turbine (process 3'-4) resulting in rotation work on the turbine shaft. In an industrial gas turbine, the shaft is connected to a generator shaft through a speed reduction gear box.

In general, gas turbines have fast starting characteristics. The improved dynamic load characteristic has made them the preferred choice for industrial applications. In the state of the art designs they are equipped with variable geometry compressors which allow wider surge and stall margins in part load applications. Topic of concern is a gas turbine working in synchronous with another gas turbine to provide the required load demand and at the same time delivering high temperature gas to a heat recovery steam generator.

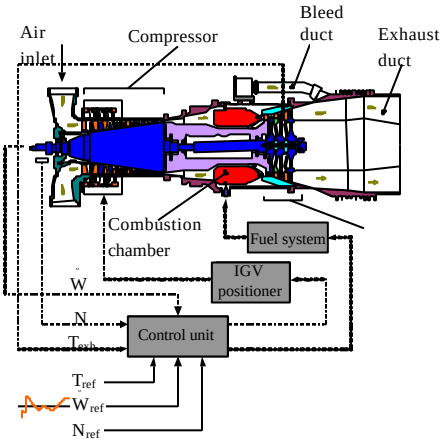

Fig. 1: Single-shaft gas turbine (Solar Turbine Inc., 2001)

During starting and for speeds lower than about 65% of the design speed, the Inlet Guide Vanes (IGVs) and Variable Stator Vanes (VSVs) are at minimum opening position; at a speed of about 98%, they open fully with the opening starting at around 65% of design speed. The latter region is identified as a variable geometry region where the IGVs and VSVs are manipulated to vary the air flow rate.

Corresponding Author: A.L. Tamiru, Department of Mechanical Engineering, Universiti Teknologi PETRONAS, Bandar Seri Iskandar, 31750, Tronoh, Perak, Malaysia

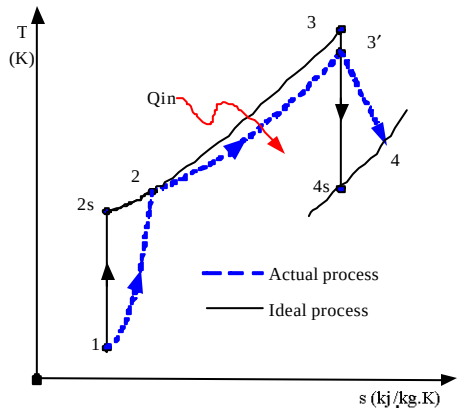

Fig. 2: Process diagram for a single-shaft gas turbine

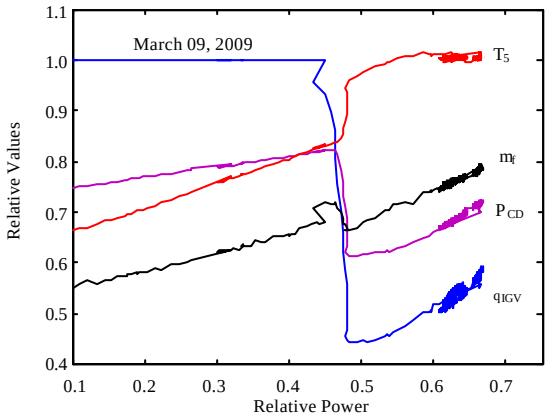

Fig. 3: Actual Operating schedule for a Single-shaft Gas Turbine Generator from Univeriti Teknologi PETRONAS GDC Plant

In a cogeneration design, the gas turbine is also expected to deliver high temperature exhaust gas. For loads higher than 50% of the rated value this requirement is achieved by a temperature controller. In this region, IGVs and VSVs are manipulated to vary the air flow rate into the compressor as per the load demand. Fuel flow rate $\dot{m}_f$ is also varied to keep temperature at the inlet of the third stage of the gas turbine (T_5) to the required set point. For a load demand lower than 50%, the gas turbine is on speed and load control. During this period the variable geometry (θ_{IGV}) is at fully open position and the state can be considered as fixed geometry region. Figure 3 shows plots of main parameters in their normalized form-each divided by their maximum value.

Dynamic studies of a gas turbine require thermodynamic models of the gas turbine components as well as details of the control system. Overall performance map instead of component performance maps are usually provided by the manufacture that made it difficult to proceed with the dynamic studies. For a variable geometry compressor, it is not practical to provide performance maps corresponding to the whole working region of the IGV and VSV settings. In energy and exergy focused parametric studies, compressor and turbine efficiencies may be assumed constant (Abam *et al*., 2011; Mahmoudi *et al*., 2009) which neglects the effect of IGV. In power plant stability studies, the simplest approach yet is to use empirical models to describe the thermodynamic part (Rowen, 1983; Zhang and So, 2000). In the study of Kakimoto and Baba (2003), the pressure ratio in the compressor and turbine are described as a function of design pressure ratio and air flow rate while the efficiencies are assumed constant. The effect of rotational speed on the pressure ratio was latter included in the models by Suzaki *et al*. (2000). An alternative approach is to use a scaling method for fixed geometry compressors and turbines (Gaudet, 2008) with extrapolation techniques applied at lower speeds. Stage-stacking techniques based on generalized stage performance curves are another widely used method (Kim *et al*., 2001). Recent techniques from computational intelligence-neural network (Zayandehroodi *et al*., 2010) and fuzzy logic (Radaideh, 2003) are also getting frequent use in the area of thermal plants. They can be applied to capture thermodynamic characteristics of the system over the whole operating region. In dynamic studies, a model needs to be simple to consume short calculation time and good enough to accommodate variable operating conditions. It must also allow the study of change in parameters like compressor inlet temperature, efficiency of the compressor, efficiency of the turbine etc.

The objective of this study is to develop compressor and turbine maps for a 5.2 MW rated industrial gas turbine whose design specifications are partially known. The research proposes the use of scaling method in the fixed geometry regions and stage-stacking method in the variable geometry region. Generalized stage and overall component performance curves from literature are used in presenting the performance characteristics. The reference map for compressors is selected after preliminary tests on the suitability of three different generalized maps. It is hoped that the resulting maps will be suitable enough to perform steady state performance and dynamic studies.

GAS TURBINE THERMODYNAMIC MODEL

In the simulation of a gas turbine the compressor and turbine are represented by performance maps. For a given

inlet conditions $\dot{m}_{air}, P_1, T_1$ and inlet fuel flow ($\dot{m}_f$) thermodynamic equations are applied to estimate properties of the working fluid at following state points. For the compressor, the temperature at the outlet (T_2) and work input requirement ($\dot{W}_c$), respectively are calculated by:

$$T_2 = T_1 + \left(\frac{T_1}{\eta_c}\right)\left(PR_c^{(\gamma-1)/\gamma} - 1\right) \quad (1)$$

$$\dot{W}_c = \dot{m}_{air}(h_2 - h_1) \quad (2)$$

where, h is enthalpy, PR_c and η_c are pressure ratio and efficiency, respectively, of the compressor corresponding to the given mass flow rate. The two values are read from specific compressor maps usually described as $PR_c = f(m_{air}, N)$ and $\eta_c = f(PR_c, N)$. Where, N is the compressor shaft speed.

The compressed air from the compressor is mixed with fuel and burned in the combustion chamber before it expands through the turbine. The temperature at the outlet of the combustion chamber ($T_{3'}$) can be estimated using combustion charts (Razak, 2007) or by an iterative approach. The energy balance around the combustor is expressed as:

$$\Delta h_{air} + \Delta h_{fuel} + LHV = (1+FAR)\,\Delta h_{hot\ gas} \quad (3)$$

where, h is the enthalpy, LHV is lower heating value of the fuel and FAR is the fuel to air ratio.

There is a pressure loss in the compressor due to the chamber resisting air flow, high level of turbulence required for combustion and heat addition. This pressure loss is considered in the model applying the following equation:

$$\frac{\Delta PR_{23'}}{P_2} = PLF \times M_{23'}^2 \gamma_2 + \left[K_1 + K_2\left(\frac{T_3}{T_2} - 1\right)\right] \quad (4a)$$

$$M_{23'} = \frac{\dot{m}_{air}}{P_2}\sqrt{\frac{R_2 T_2}{\gamma_2}} \quad (4b)$$

where, PLF is the pressure loss factor; $M_{23'}$ is the dimensionless flow; K_1 and K_2 are constants for the cold loss and hot loss of the combustor, respectively. Then from the pressure loss and inlet pressure:

$$P_3 = P_2 - \Delta P_{23'} \quad (5)$$

The hot gas temperature leaving the turbine (T_4) and the power transferred to the turbine shaft are expressed as:

$$T_4 = T_{3'} - T_{3'}\eta_t\left(1 - \left(\frac{1}{PR_t}\right)^{(\gamma_g-1)/\gamma_g}\right) \quad (6)$$

$$\dot{W}_t = (\dot{m}_{air} + \dot{m}_f)(h_{3'} - h_4) \quad (7)$$

where, h is enthalpy of the hot gas; $\eta_t = f_1(PR_t, N)$ and PR_t are isentropic efficiency and pressure ratio, respectively, of the turbine. The pressure at the outlet of the turbine P_4 is limited to less than 105.825 kPa. Using this value, the pressure ratio is calculated and used in $(m_{air}+m_f) = f_2(PR_t, N)$ to check if the mass balance is satisfied.

The following is assumed for the electric power at the generator terminal:

$$\dot{W}_{ele} = \frac{1}{\eta_{ele}}\left(\dot{W}_t - \frac{\dot{W}_c}{\eta_m}\right) \quad (8)$$

where, η_m and η_{ele} are mechanical efficiency and electrical efficiency, respectively.

In the first step of performance map calculation, Eq. 1-8 are applied iteratively to determine estimated design point parameters. At each state point variation of specific heats with temperatures are taken into consideration.

Most of the time, Heat Rate (HR), Lower Heating Value (LHV) of the fuel and exhaust flow rate ($\dot{m}_{exh}$) are provided. In that case, the following equations are applied to obtain the fuel flow rate and air mass flow rate, respectively:

$$\dot{m}_f = \frac{\dot{W}_{ele} \times HR}{LHV} \quad (9)$$

$$\dot{m}_{air} = \dot{m}_{exh} - \dot{m}_f \quad (10)$$

Once the component design parameters are determined, scaling and stage-stacking methods are applied to generate the performance maps. Off-design analysis is just solving the same set of Eq. 1-8 satisfying the matching conditions-conservation of mass and power.

Scaling method: For a compressor, there are three available performance calculation techniques: scaling method, stage-stacking method and blade element method (Johnsen and Bullock, 1965). Among the three, scaling method is the easiest. But the inherent simplicity has the drawback of demanding a suitable reference map. Besides,

it is not suitable for studying variable geometry compressors from the point of view of understanding the stage interaction inside the compressor. Scaling method is good enough if the interest of the analyst is to understand the compressor as a black box. This is true for the case of fixed geometry compressors. As will be demonstrated in the results and discussion section, the accuracy of the method is largely dependent on the shapes of the reference maps. Scaling method overlooks compressibility effect. Modified versions of the scaling method have been suggested recently (Kong and Ki, 2007; Kong *et al*., 2003). The main idea in the scaling method is that performance map of a compressor can be generated if the design conditions $\dot{m}_{des}$, PR_{des} and η_{des} are known. The basic equations for the scaling method are:

Pressure ratio:

$$PR = \left(\frac{PR_{des} - 1}{PR_{map,\,des} - 1}\right)(PR_{map} - 1) + 1 \tag{11}$$

Mass flow rate:

$$\dot{m} = \left(\frac{\dot{m}_{des}}{\dot{m}_{map,\,des}}\right)\dot{m}_{map} \tag{12}$$

Efficiency:

$$\eta_{isen} = \left(\frac{\eta_{des}}{\eta_{isen,des}}\right)\eta_{isen,map} \tag{13}$$

where, $PR_{map,\,des}$ and PR_{map} are design pressure ratio and off-design pressure ratio for the reference map; $\dot{m}_{map,\,des}$ and $\dot{m}_{map}$ are design mass flow rate and off-design mass flow rate for the reference map; $\eta_{isen,\,des}$ and $\eta_{isen,\,map}$ are design efficiency and off-design efficiency, respectively, of the reference map. For generating the compressor performance maps using the scaling method, multi-stage compressor maps from three different sources (Converse and Giffin, 1984; Johnsen and Bullock, 1965; Saravanamuttoo and MacIsaac, 1983) will be considered. The first set of maps were used to study a two-spool industrial gas turbine (Zhu and Saravanamuttoo, 1992).

For turbines, the easiest method is to assume that the turbine is choked and the corresponding efficiency is constant. If that is not good enough, Stodola ellipse equation (Dixon, 2005) or one-dimensional nozzle equation (Ordys *et al*., 1994) may be applied. The third option is to use Ainley and Mathieson (1951) method. This method, however, requires geometric data which is hardly available. In this paper, scaling method that demands relatively little information at design point is considered.

Stage-stacking method: In the stage stacking method, generalized stage performance curves are used in order to develop overall compressor performance. Based on a flow coefficient ϕ calculated at the inlet of a stage, pressure ratio ψ and efficiency η are read from generalized curves and used to estimate for outlet pressure and temperature of the stage. The total pressure and temperature at the outlet of the preceding stage are considered as an input to the following stage. The calculations are repeated covering all the stages in the compressor. The properties at the outlet of the last stage will be considered as the properties of the compressor. The relevant equations are as described below:

Flow coefficient:

$$\phi = \frac{C_a}{U} \tag{14}$$

Pressure coefficient:

$$\psi = \left(\frac{C_p T_{os}}{U^2}\right)(PR^{(\gamma-1)/\gamma} - 1) \tag{15}$$

Temperature coefficient:

$$\zeta = \frac{C_p \Delta T_{os}}{U^2} \tag{16}$$

Efficiency:

$$\eta = \left(\frac{C_p T_{os}}{\Delta T_{os}}\right)(PR^{(\gamma-1)/\gamma}) = \frac{\psi}{\zeta} \tag{17}$$

where, C_a is the stage inlet axial velocity, U is the tangential blade speed, T_{os} is stage inlet air total temperature, ΔT_{os} is stage total temperature rise, C_p is specific heat at constant pressure and γ is ratio of specific heats.

Stage-stacking procedure is suitable to develop performance maps for fixed as well as variable geometry compressors. The first proposed stage stacking method was based on the stage performance map of a single stage compressor or fan. Latter it was improved by introducing

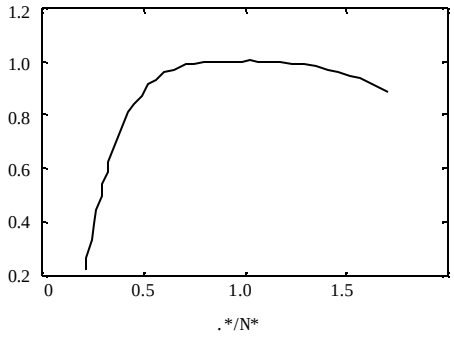

Fig. 4: Graph of stage normalized efficiency versus ratio between temperature coefficient and flow coefficient (Howell and Bonham, 1950)

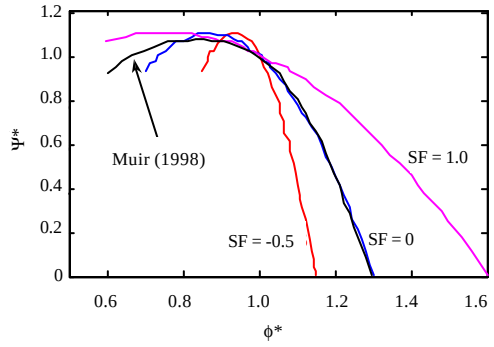

Fig. 5: Plot of normalized pressure coefficient versus normalized flow coefficient $\psi^* = f_\psi(\phi^*, SF)$ (Spina, 2002)

generalized stage performance curves. Ratios of each characteristic parameter (Eq. 14-17) and the value of the same parameter at the point of maximum efficiency are used to define a point on the generalized curves. Figure 4 shows the generalized efficiency curve as developed by Howell and Bonham (1950). The other curve required for stage-stacking calculation is the ψ^* verse ϕ^* plot (Fig. 5). This was developed by Muir (1988) assembling a number of openly published stage data on pressure ratio. The concept of Shape Factor (SF) was then introduced by Spina (2002) to obtain a number of generalized curves covering all the data points calculated by Muir (1988). The corresponding equation becomes:

$$\psi^* = \psi^*_{max} - \frac{\psi^*_{max} - 1}{[\phi^*_{\psi_{max}} + SF(\phi^*_{\psi_{max}} - 1) - 1]^2}[\phi^*_{\psi_{max}} + SF(\phi^*_{\psi_{max}} - 1) - \phi^*]^2 \quad (18)$$

where:

$$\phi^* = \left(\frac{\phi}{\phi_{ref}}\right);\ \psi^* = \left(\frac{\psi}{\psi_{ref}}\right);\ \psi^*_{max} = 1.115;\ \phi^*_{\psi_{max}} = 0.835.$$

The normalized isentropic efficiency and total temperature equations are given by:

$$\eta^* = \left(\frac{\eta}{\eta_{ref}}\right) \quad (19a)$$

$$\zeta^* = \left(\frac{\zeta}{\zeta_{ref}}\right) \quad (19b)$$

In order to obtain stage characteristics of a given compressor the shape factor is estimated by minimizing the sum of squares of errors between calculated and given performance parameter, for instance compressor pressure ratio.

In a variable geometry compressor, IGVs and VSVs are adjusted to cope with the variation of speed and gas turbine load. In that case, each new setting of the blades results in a new stage characteristic. From velocity triangle of a rotating compressor blade (Fig. 6a) and assuming constant axial flow velocity and mean rotor speed and from equation of energy balance for the rotor:

$$\frac{1}{\phi} = \tan\alpha_1 + \tan\beta_1 \text{ and} \quad (20)$$

$$\zeta = 1 - \phi\,(\tan\alpha_1 + \tan\beta_2) \quad (21)$$

Assuming that the IGVs and VSVs are adjusted such that the relative flow angles are constant and equal to the design point angles (Fig. 6b), Eq. 20 can be written in a form suitable to find generalized performance curves at off-design IGVs and VSVs setting:

$$\frac{1}{\phi} = \left(\frac{1}{\phi} - \tan\alpha_1\right)_{des} + \tan\alpha_1 \quad (22)$$

The same set of assumptions leads to the conclusion that efficiency is constant. This makes sense for the pressure losses across the rotor blades are at minimum if the angle of incidence is adjusted such that the flow angle is unaffected. The resulting equation between ϕ and ψ will be:

$$\psi = \left(\frac{\psi}{\phi}\right)_{des}\phi \quad (23)$$

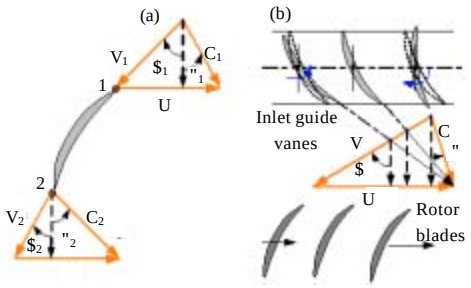

Fig. 6: Compressor blades: (a) velocity triangles (b) IGV setting

RESULTS AND DISCUSSION

The results from application of the proposed methods are presented here. The first sets of maps are modeled by scaling method. As mentioned in the discussion of the scaling method, data from three different sources will be used as reference data. Fig. 7 shows the difference in the shapes of the three selected reference maps. At the corrected design speed ($N/N_d = 1$), the three maps seem overlapping in a certain region. For speeds other than the design point, the maps are hardly close to each other. These set of maps are chosen arbitrarily to see if random selection of a compressor map in a certain application is acceptable at all the times.

The first axial compressor considered for testing the suitability of the three reference maps is taken from (Budinger and Thomson, 1952). The compressor is a 10 stage axial flow compressor with mass flow rate $\dot{m}_d = 20\ kg\ sec^{-1}$, pressure ratio PR_d = 12.4, efficiency $\eta_d = 0.86$ and shaft speed $N_d = 14000$ rpm. The comparison between experimental data of the compressor and the maps generated based on the three reference maps are shown in Fig. 8. The scaled maps predicted different points except for the few points closely predicted by Johnsen's Map in the lower speed regions.

The second axial compressor selected for examining the same set of reference maps is obtained from (Geye *et al*., 1953) . The compressor is designed for a mass flow rate of $\dot{m}_d = 29.48\ kg\ sec^{-1}$, pressure ratio of PR_d = 10.26, isentropic efficiency of η_d = 0.86 and rotational speed of N_d = 13380 rpm. As presented in Fig. 9, at the design speed of the compressor, the prediction by the three reference maps are somehow in agreement. For the off-design speed, the only reference map that may be considered is the Johnsen's map.

The third test compressor map is a 16 stage compressor taken from Medeiros *et al*. (1951). It has the design flow capacity of $\dot{m}_d = 70.3068\ kg\ sec^{-1}$ and pressure ratio of PR_d = 8.75 for a speed of N_d = 6100 rpm and efficiency η_d = 0.83. Similar to the previous compressors the same set of reference compressors maps were applied to predict off-design characteristics of the compressor. The resulting curves are depicted in Fig. 10. At 80% of the design speed, Saravanamutto's map seems predicting the

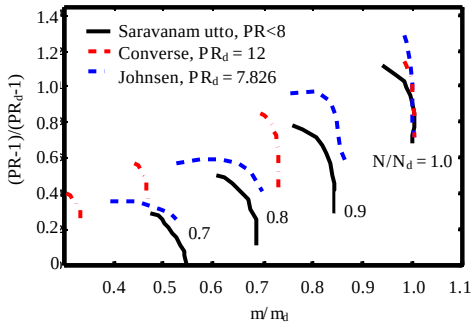

Fig. 7: Normalized reference compressor performance maps

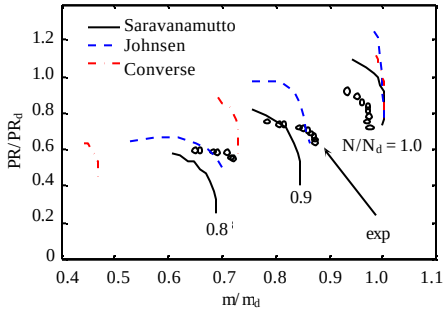

Fig. 8: Performance map of a 10-stage axial compressor ($\dot{m}_d = 20\ kg\ sec^{-1}, PR_d = 12.4, N_d = 14000 rpm$) (Budinger and Thomson, 1952)

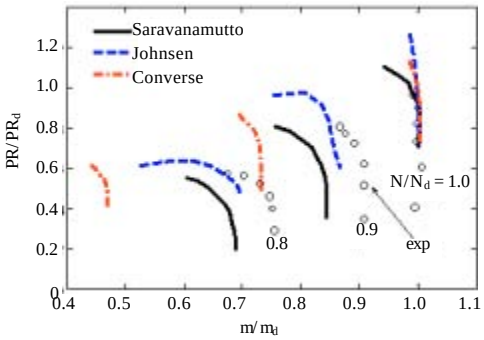

Fig. 9: Performance map of an 8 stage compressor (Geye *et al*., 1953) ($\dot{m}_d = 29.48\ kg\ sec^{-1}, PR_d = 10.26, N_d = 13380 rpm$)

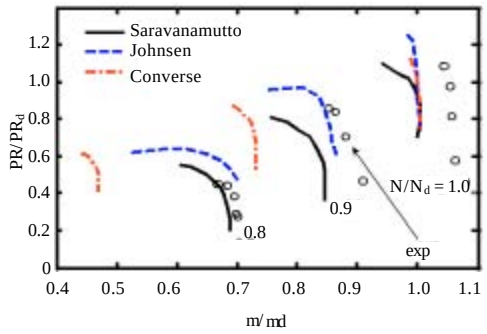

Fig. 10: Performance map of a 16 stage compressor (Medeiros *et al.*, 1951) ($\dot{m}_d = 70.3.68\ kg\ sec^{-1}, PR_d = 8.75, N_d = 6100\ rpm$)

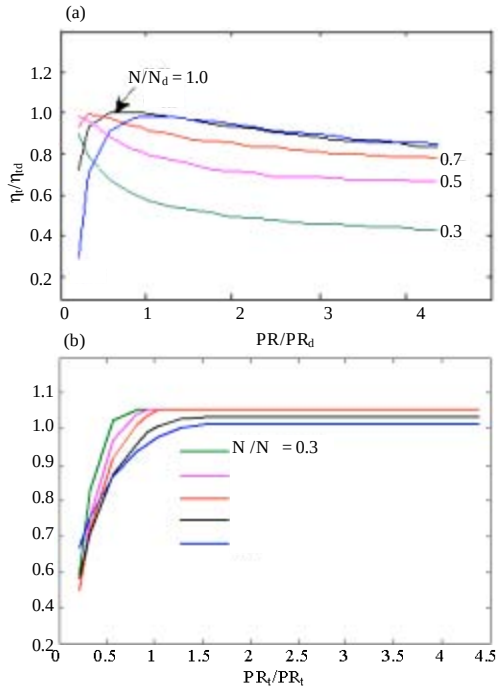

Fig. 11: Performance maps of a 3-stage turbine: (a) Normalized efficiency versus normalized pressure ratio (b) Normalized mass flow rate versus normalized pressure ratio ($\dot{m}_d = 21.7\ kg\ sec^{-1}, PR_d = 10, N_d = 14944 rpm$)

performance accurately. Except that, the rest of the predictions are far from being acceptable for further analysis.

From the presented tests, it is observed that even for pressure ratios closer to the reference map pressure ratio the resulting prediction may not be as accurate as expected. Therefore, having this problem from the simplest technique known and with the scant information available from manufactures catalogue, the task of finding a suitable map using this method is too much of an out of option procedure than other wise.

Table 1: Design specification of solar gas turbine

Parameters		Taurus 60s-7301	Engine
Speed (rpm)			14944
Electric Power (kW)			5200
Heat Rate (kJ/kWh)			11730
Compressor		12-stage axial	
	*Inlet air flow (kg sec^{-1})		21.364
	*Pressure ratio		11
Turbine		3-stage axial	
	*Inlet Temperature (°C)		1035
	*Exit Temperature (°C)		505
	*Pressure Ratio		10.053

*Calculated values

The present work suggested scaling method for the fixed geometry region and stage stacking method for the variable geometry region. The stage stacking method is more involved as it follows a design procedure based on carefully decided design parameters. However, as demonstrated latter, the accuracy is much better than scaling method.

After studying the importance of choosing a geometrically suitable reference map for predicting the performance of an axial compressor based on the scaling method, the technique was applied to the components of a 5.2 MW Solar gas turbine. Manufacturer supplied overall parameters as indicated in Table 1 are used for the calculations. To determine the missing design information regarding the 12 stage axial flow compressor and the 3 stage turbine, Eq. 1-10 were solved in an iterative way with the objective of minimizing sums of Squares of Relative Errors (SSRE) given by the following equation:

$$SSRE = \left(1 - \frac{\hat{P}_2}{P_{2a}}\right)^2 + \left(1 - \frac{\hat{W}_{ele,a}}{W_{ele,a}}\right)^2 \quad (24)$$

where, P_{2a} is design point compressor discharge pressure and $\hat{W}_{ele,a}$ is the power at the generator terminal. The error is minimized varying isentropic efficiencies of the compressor and turbine, respectively. The design point discharge pressure is read from overall performance map of the gas turbine provided by the manufacturer. Results of the optimization calculation are given in Table 1.

From the optimized result, the turbine appeared to have exhaust gas flow rate of $\dot{m}_d = 21.7\ kg\ sec^{-1}$ and a pressure ratio of $Pr_d = 10$ while the compressor is featured by a mass flow rate of $\dot{m}_d = 21.364\ kg\ sec^{-1}$ and pressure ratio of $PR_d = 11$. The performance maps developed based on the calculated design values are portrayed in Fig. 11 and 12. As a reference, a turbine map from

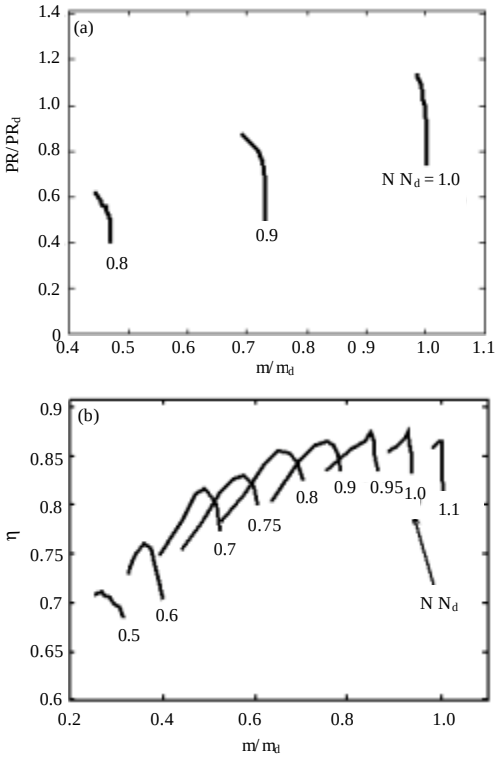

Fig. 12: Performance maps of a 12-stage compressor: (a) Normalized pressure ratio versus normalized mass flow rate (b) Efficiency versus normalized mass flow rate ($\dot{m}_d = 21.364$ kg sec^{-1}, $PR_d = 11$, $N_d = 14944$ rpm)

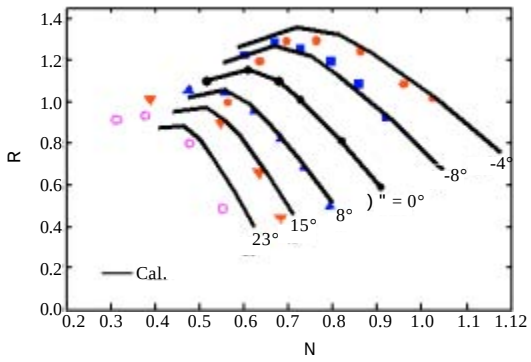

Fig. 13: Plot of pressure coefficient versus flow coefficient for a variable geometry compressor (Kim *et al*., 2001; Song *et al*., 2000)

Converse (1984) is chosen for applying the scaling method attributed closer design pressure ratio to the pressure ratio of the Solar Turbine.

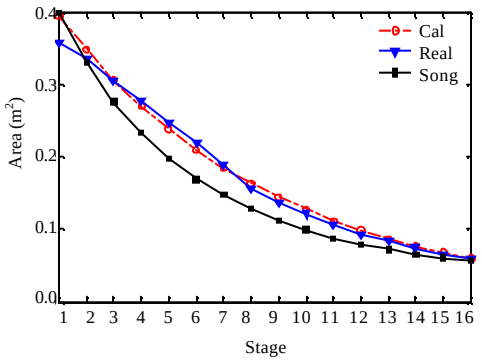

Fig. 14: Stage inlet flow area of a 16-stage compressor (Muir, 1988)

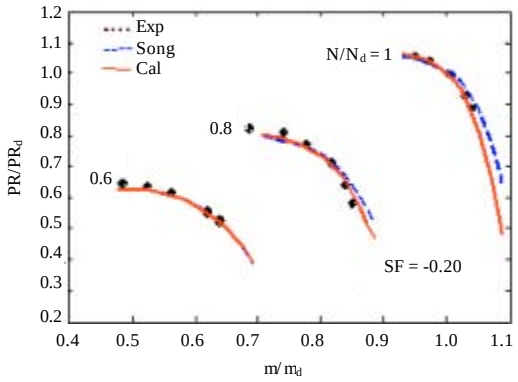

Fig. 15: Plot of normalized pressure ratio versus normalized mass flow rate for a 3-stage axial compressor (Kashiwabara *et al*., 1986) ($\dot{m}_d = 16.1$ kg sec^{-1}, $PR_d = 2.2$, $N_d = 17000$ rpm)

In applying the stage-stacking method, Eq. 22 and 23 are first validated by experimental data taken from (Kim *et al*., 2001). As indicated in Fig. 13, the results from the two equations are in good agreement with the experimental data.

Stage-stacking method relies on geometric data. However, this information is not available for proprietary reasons. In this paper, a general design procedure with design conditions decided based on data from well established literature are adapted. The following parameters are assumed for design point calculation.

- Axial velocity : 150 m sec^{-1}
- Inlet temperature : 288.15 K
- Inlet pressure : 101.325 kPa
- Polytropic efficiency : 0.89
- Inlet flow angle : 15°

For validating the geometry calculation, actual dimensions for 16 stage axial compressor taken from Muir (1988) is compared with the geometry calculated using to the above input parameters. As indicated in Fig. 14, the real design and the calculation result match quite closely. The stage-stacking method, before it is applied to the Solar Turbine, is also tested by predicting off-design performance characteristics of a 3 stage axial flow compressor taken from Kashiwabara *et al*. (1986). As shown in Fig. 15, the calculated result agrees well with the experimental data as compared to other similar work (Song *et al*., 2000).

CONCLUSION

In this study, we have developed gas turbine component maps based on partially known design information. At the start, three reference maps from different sources have been tested to verify if random selection of reference maps could be used for generating characteristic curves through scaling method. After testing the reference maps by three other actual compressor maps, the scaling method is applied to Solar Taurus 60s gas turbine whose overall design information is partially known. Based on the cases tested, the following conclusions have been reached:

- Having partially known overall design information, the application of scaling method requires care in the selection of the reference map. It was observed that even for the case where the design pressure ratios of the reference and the new compressor are closer, accurate off design point performance prediction may not be granted
- As compared to the scaling method, the stage stacking method well matches the experimental data. The only drawback to this method is the need for design point calculation

The next task to the presented work is to test the generated performance maps in actual overall performance prediction of the gas turbine generator.

ACKNOWLEDGMENT

The authors acknowledge the support by Universiti Teknologi PETRONAS for providing all the resources sought by the research.

REFERENCES

Abam, F.I., D.C. Onyejekwe and G.O. Unachukwu, 2011. The effect of ambient temperature on components performance of an in-service gas turbine plant using exergy method. Singapore J. Sci. Res., 1: 23-37.

Ainley, D.G. and G.C.R. Mathieson, 1951. A method of performance estimation for axial-flow turbines. ARC R.&M. No. 2974. http://oai.dtic.mil/oai/oai?verb=getRecord&metadataPrefix=html&identifier=ADA950664.

Budinger, R.E. and R.A. Thomson, 1952. Investigation of a 10-stage subsonic axial-flow research compressor II: Preliminary analysis of over-all performance. NACA RM ES2CO4.

Converse, G.L. and R.G. Griffin, 1984. Extended parametric representation of compressor fans and turbines. Volume 1: CMGEN User's Manual. NASA-CR-174645. manual.http://ntrs.nasa.gov/archive/nasa/casi.ntrs.nasa.gov/19860014465_1986014465.pdf

Coverse, G.L., 1984. Extended parametric representation of compressor fans and turbines. Volume 2: Part User's Manual (Parametric Turbine). NASA-CR-174646.

Dixon, S.L., 2005. Fluid Mechanics, Thermodynamics of Turbomachinery. 5th Edn., Butterworth-Heinemann, Burlington, MA, USA.

Gaudet, S.R., 2008. Development of a dynamic modeling and control system design methodology for gas turbines. Ph.D. Thesis, Carleton University, Canada.

Geye, R.P., R.E. Budinger and C.H. Voit, 1953. Investigation of a high-pressure-ratio eight-stage axial-flow research compressor with two transonic inlet stages II: Preliminary analysis of over-all performance. NACA RM E53J06.

Howell, A.R. and R.P. Bonham, 1950. Overall and stage characteristics of axial flow compressor. Proc. IMechE, 163: 235-248.

Johnsen, I.A. and R.O. Bullock, 1965. Aerodynamic design of axial-flow compressors. No. NASA SP-36. http://openlibrary.org/books/OL5965028M/Aerodynamic_design_of_axial-flow_compressors.

Kakimoto, N. and K. Baba, 2003. Performance of gas turbine-based plants during frequency drops. IEEE Trans. Power Syst., 18: 1110-1115.

Kashiwabara, Y., Y. Matsuura, Y. Katoh, N. Hagiwara, T. Hattori and K. Tokunaga, 1986. Development of a high-pressure-ratio axial flow compressor for a medium-size gas turbine. J. Turbomachinery, 108: 233-239.

Kim, J.H., T.W. Song, T.S. Kim and S.T. Ro, 2001. Model development and simulation of transient behavior of heavy duty gas turbines. J. Eng. Gas Turbines Power, 123: 589-594.

Kong, C. and J. Ki, 2007. Components map generation of gas turbine engine using genetic algorithms and engine performance deck data. J. Eng. Gas Turbines Power, 129: 312-317.

Kong, C., J. Ki and M. Kang, 2003. A new scaling method for component maps of gas turbine using system identification. J. Eng. Gas Turbines Power, 123: 979-985.

Mahmoudi, S.M.S., V. Zare, F. Ranjiban and L. Garooci-Farshi, 2009. Energy and exergy analysis of simple and regenerative gas turbine inlet air cooling using absorption refrigeration. J. Applied Sci., 9: 2399-2407.

Medeiros, A., D.C. Guentert and J.E. Hatch, 1951. Performance of J35-A-23 compressor I: over-all performance characteristics at equivalent speeds from 20 to 100 percent of design. NACA-RM-E50J17.

Muir, D.E., 1988. Axial Flow Compressor Modelling for Engine Health Monitoring Studies. Carleton University, Canada.

Ordys, A.W., A.W. Pike, M.A. Johnson, R.M. Katebi and M.J. Grimble, 1994. Modelling and Simulation of Power Generation Plant. Springer-Verlag, London.

Radaideh, O.Y., 2003. Selection of load node model in power systems: Fuzzy logic approach. Inform. Technol. J., 2: 148-153.

Razak, A.M.Y., 2007. Industrial Gas Turbines Performance and Operability. Woodhead Publishing Ltd., CRC Press LLC, Cambridge, England.

Rowen, W.I., 1983. Simplified mathematical representations of heavy-duty gas turbines. J. Eng. Power, 105: 865-869.

Saravanamuttoo, H.I.H. and B.D. MacIsaac, 1983. Thermodynamic model for pipeline gas-turbine diagnostics. Trans. ASME J. Eng. Power, 105: 875-884.

Solar Turbine Inc., 2001. Solar turbine training manual. Solar Turbine Incorporated, San Diego, CA.

Song, T.W., J.H. Kim, T.S. Kim and S.T. Ro, 2000. Effective Performance Prediction of Axial Flow Compressors using a Modified Stage-Stacking Method. The Korean Society of Mechanical Engineers, South Korea.

Spina, P.R., 2002. Gas turbine performance prediction by using generalized performance curves of compressor and turbine stages. ASME Paper No. GT-2002-30275.

Suzaki, S., K. Kawata, M. Sekoguchi and M. Goto, 2000. Mathematical model for a combined cycle plant and its implementation in an analogue power system simulator. IEEE Power Eng. Soc. Winter Meeting, 1: 416-421.

Zayandehroodi, H., A. Mohamed, H. Shareef and M. Mohammadjafari, 2010. Automated fault location in a power system with distributed generations using radial basis function neural networks. J. Applied Sci., 10: 3032-3041.

Zhang, Q. and P.L. So, 2000. Dynamic modelling of a combined cycle plant for power system stability studies. Power Eng. Soc. Winter Meeting IEEE, 2: 1538-1543.

Zhu, P. and H.I.H. Saravanamuttoo, 1992. Simulation of an advanced twin-spool industrial gas turbine. J. Eng. Gas Turbines Power, 114: 180-185.